Catalysis Letters (2023) 153:1475–1482
https://doi.org/10.1007/s10562-022-04081-5

# Highly Dispersed Cobalt Centers on UiO-66-$NH_2$ for Photocatalytic $CO_2$ Reduction

**Songchang Hu[1] · Zesheng Deng[1] · Mingyang Xing[1] · Shiqun Wu[1] · Jinlong Zhang[1,2]**

Received: 24 April 2022 / Accepted: 9 June 2022 / Published online: 1 July 2022


## Abstract

Metal–organic frameworks (MOFs) are potential photocatalytic materials for $CO_2$ reduction, however, still limited by their low efficiency. In this work, cobalt decorated UiO-66-$NH_2$ (xCoNU, x presents the mass friction of cobalt) were successfully synthesized through an economic $NaBH_4$ treating method and applied for $CO_2$ photocatalytic reduction. It was confirmed that cobalt worked as the active site in the system, and an optimized CO yielding rate of 1.93 mmol $g^{-1}$ $h^{-1}$ in 3 h was achieved on 5CoNU, which is 10.2 times higher than that of UiO-66-$NH_2$. Characterization results revealed that the highly dispersed cobalt in xCoNU accelerates the charge separation and electron transport in the photocatalytic system, improving the photocatalytic $CO_2$ reduction performance. This work provides a simple and convenient method to modify MOFs with metal cocatalyst, and is expected to advance the development of efficient $CO_2$ photoreduction catalysts.

## Graphical Abstract

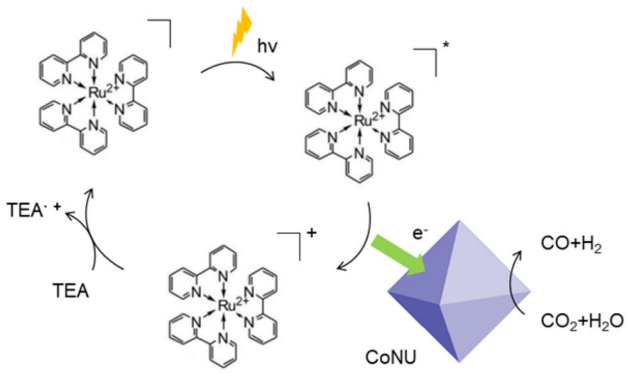


**Keywords** $CO_2$ reduction · Photocatalysis · Cobalt · UiO-66-$NH_2$

✉ Shiqun Wu
wushiqun@ecust.edu.cn

✉ Jinlong Zhang
jlzhang@ecust.edu.cn

[1] Shanghai Engineering Research Center for Multi-Media Environmental Catalysis and Resource Utilization, Key Laboratory for Advanced Materials and Joint International Research Laboratory of Precision Chemistry and Molecular Engineering, School of Chemistry and Molecular Engineering, East China University of Science and Technology, 130 Meilong Road, Shanghai 200237, People's Republic of China

[2] School of Chemistry and Chemical Engineering, Yancheng Institute of Technology, Yancheng 224051, People's Republic of China

## 1 Introduction

Converting $CO_2$ into renewable energy via artificial photosynthesis is ideal pathway for addressing the escalating energy shortages and climate changes at the same time [1–4]. However, though countless effort has been paid till today, the solar-driven $CO_2$ conversion is still suffered a low efficiency, which should be attributed to the high chemical stability of $CO_2$ molecules and the fast recombination of photogenerated charge carriers [5–7]. These facts make the design and construction of highly efficient catalyst essential for further application of photocatalytic $CO_2$ conversion [8–10]. Metal–organic frameworks (MOFs) are a class of crystalline porous materials consisting of tunable multitopic organic linkers and metal-based nodes [11–13]. With their typically high accessible surface area, MOFs are promising candidates for a wide range of applications including gas capture, separation, and storage [14–17]. It was fessible to modify MOFs with cocatalysts, and the modified MOFs exhibited great potential in photocatalysis such as pollutant degradation, hygogen evolution and $CO_2$ reduction as a type of semiconductor-like materials [18–23]. For example, controllable manipulation of metal composites or single atoms have been used as MOF catalyst engineering strategies in recent years [24–27]. It is found that some MOFs such as UiO-66-$NH_2$ with amine groups can have strong coordination with metal ions, which could be beneficial to achieving higher dispersion of metal atoms [28–30]. Such atomic modification with high atomic utilization efficiency often gives impressive activity in heterogeneous photocatalysis with MOF for introducing considerable reactive sites and it also offers an opportunity to promote the separation of exicted electrons and holes during the photocatalysis process.

Previous works have proven that cobalt is a promising catalytic center for $CO_2$ photocatalytic reduction reaction [31–33]. Coordinatively unsaturated Co sites were proved to be able to accept excited electrons from substrate [34], which greatly enhanced the separation of photoinduced electrons and holes. It is also found that the Co sites have a great promotion effect on the adsorption and activation of $CO_2$ by strong interaction between Co 3d electrons and C 2p electrons of adsorbed $CO_2$, which could hence active $CO_2$ effectively [35]. Notably, the application of cobalt cocatalyst was limited by the low dispersion on traditional semiconductors. On the other hand, as in the construction of Co modified MOFs materials, expansive linkers or metal–organic complexes are widely used. Regardless the good activity those catalysts have, it is not economical for further application. Herein, in order to increase the atomic utilization of Co, we realize the decoration of highly dispersed Co into UiO-66-$NH_2$ through an economic $NaBH_4$ treating method. With the promoted dispersion of cobalt, the obtained xCoNU photocatalyst exhibited outstanding catalytic performance. The CO generation rate was up to 1.93 mmol $g^{-1}$ $h^{-1}$, with TON of 38 within 3 h, which is 10.2 times higher than that of UiO-66-$NH_2$. In addition, the improved photocatalytic performance caused by the introduction of cobalt has also been studied in detail. This work provides a promising approach to engineering the actives sites on MOF materials for solar-driven $CO_2$ conversion.

## 2 Experiment Section

### 2.1 Preparation of UiO-66-$NH_2$

UiO-66-$NH_2$ (noted as NU66) was synthesized by a solvothermal method. 0.24 g $ZrCl_4$, 3.75 g benzoic acid and 0.18 g 2-amino-1, 4-benzenedicarboxylic acid ($NH_2$-BDC) were added into 60 mL dry dimethyl formamide (DMF). The mixture was sonicated and stirred for 10 min to achieve a homogenous solution. Then the solution was transferred into a 100 mL stainless autoclave with Teflon liner and heated at 120 °C for 24 h. After cooling down to room temperature, the resultant suspension was filtered, washed with DMF and methanol respectively. The final product was dried under vacuum for 12 h at 50 °C.

### 2.2 Preparation of xCoNU

Series of xCoNU (x presents the theoretical Co loading weight percentage) was obtained by $NaBH_4$ treating method. Typically, for the synthesis of 1CoNU, 0.1 g NU66 was firstly dispersed in 35 mL acetonitrile (MeCN). Acetonitrile solution of $CoCl_2{\cdot}6H_2O$ dissolved (4 mg, 5 mL) was then added into the suspension, and the mixture was kept stirring for 30 min. Afterward acetonitrile solution of $NaBH_4$ (6.8 mg, 10 mL) was slowly dropped into the mixture. To promote a complete reaction, the mixture was kept for another 10 min stirring. Then precipitate was collected by centrifugation and washed by acetonitrile several times. The final product was dried under vacuum without heat. 2CoNU, 5CoNU, 7CoNU and 10CoNU were synthesized by similar method which only scaled up the amount of $CoCl_2{\cdot}6H_2O$ and $NaBH_4$ during reaction.

### 2.3 Characterizations

TEM images were recorded by a JEM-2100 equipped with fast Fourier transformation (FFT). The crystallinity of samples was characterized by Rigaku D/MAX 2550 diffraction meter with Cu K radiation ($\lambda = 1.5406$ Å) at 40 kV and 40 mA. The surface chemical states of samples were

determined by high-resolution XPS (PerkinElmer PHI 5000C ESCA system: Al Kα radiation, operated at 250 W). Ultraviolet–visible (UV–vis) diffuse reflectance spectra were recorded by a UV–vis spectrophotometer (UV-2600, Shimadzu). The charge separation efficiency of all samples was evaluated on a luminescence spectrometer (Cary Eclipse) with the excitation wavelength at 315 nm. The charge transfer efficiency of samples was evaluated by Electrochemical Impedance Spectroscopy (EIS) on a Zennium electrochemical station with a three-electrode cell. Time-resolution photoluminescence (TRPL) spectra was performed on an Edinburgh Analytical Instruments FLS 980 coupled with a time-correlated single-photo-counting system at room temperature.

### 2.4 $CO_2$ Photocatalytic Reduction (CO2PR) Evaluation

In the typical photocatalytic $CO_2$ reduction reaction, 5 mg of catalyst, 5 mg of $[Ru(bpy)_3]Cl_2{\cdot}6H_2O$ (abbreviated as **Ru**, bpy = 2′2-bipyridine), 1.0 mL of triethylamine (TEA), 1.0 mL of $H_2O$ and 8.0 mL of acetonitrile were added into a homemade quartz reactor with total volume of 200 mL. Then, high purity $CO_2$ was introduced into the reactor with a partial pressure of 1.0 atm. A 300 W Xe lamp with a AM1.5 cut-off filter was used as the light source. During the reaction, the reaction system was viciously stirred by magnetic stirrer to ensure a homogeneous gaseous atmosphere. The temperature of the reaction system was kept at 25 °C by condensate water. The gaseous mixture was analyzed by a gas chromatograph (GC2014, Shimadazu, carrier gas: Ar) equipped with a thermal conductivity detector (TCD) and a flame ionization detector (FID) every half an hour. The GC was equipped with 3 columns: an FFAP column and a PN for the pre-separation of the gas, and a 13X column for the separation of $H_2$, $O_2$, $CH_4$, CO and $H_2$. $H_2$ was measured by TCD. $CH_4$ was measured by FID, while CO was converted to $CH_4$ by a methanation reactor first and then analyzed by the FID.

## 3 Results and Discussion

The morphology of as-synthesized UiO-66-$NH_2$ based catalysts was analyzed by TEM. As shown in Fig. 1A (UiO-66-$NH_2$) and Fig. 1B (5CoNU), no significant change for the MOF was found after the introducing of Co, which suggested that UiO-66-$NH_2$ was feasible for modification. The XRD patterns of blank UiO-66-$NH_2$ and 5CoNU were shown in Fig. S1. Typical UiO-66-$NH_2$ patterns were obtained and no significant crystallinity change was found after the Co modification [36]. On the other hand, no peaks belonging to cobalt-related species can be sighted, possibly due to the low loading amount of cobalt. Given that directly reducing $CoCl_2$ in the same condition only resulted in an amorphous product, it was also possible that Co species in 5CoNU stayed amorphous.

The loading amount of cobalt in xCoNU series samples was verified by ICP-AES. As listed in Table 1, the actual loading amount of Co in samples was all around 65% of calculated result, indicating a similar Co reduction level in xCoNU. Notably, when replacing UiO-66-$NH_2$ with UiO-66

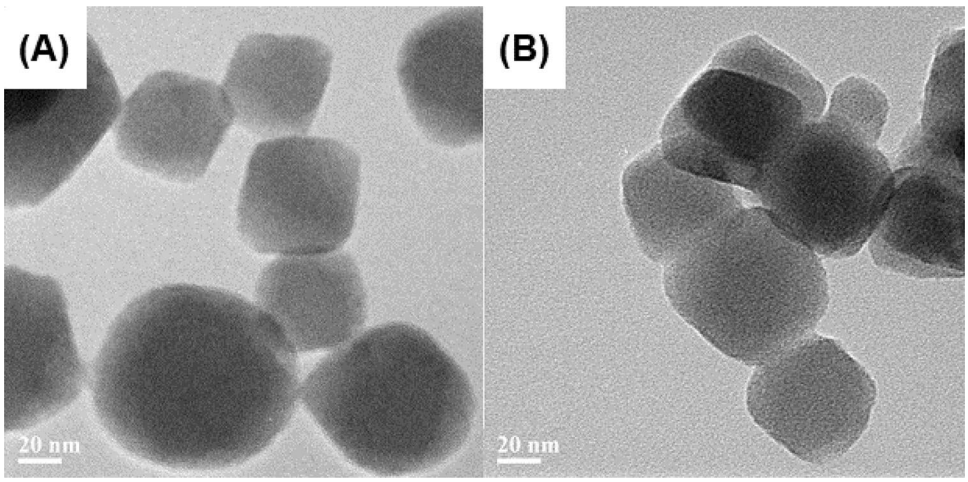


**Fig. 1** TEM images of **A** NU66, **B** 5CoNU

**Table 1** Cobalt content in xCoNU (x = 1, 2, 5, 7, 10) and 5CoUiO-66

| Samples | 1CoNU | 2CoNU | 5CoNU | 7CoNU | 10CoNU | 5CoUiO-66 | 5CoNU (water) |
|---|---|---|---|---|---|---|---|
| Co wt% (calculated) | 1.0 | 2.0 | 5.0 | 7.0 | 10.0 | 5.0 | 5.0 |
| Co wt% (ICP-AES) | 0.62 | 1.32 | 3.61 | 4.76 | 6.32 | 2.83 | 0.55 |

which lacks $–NH_2$ to synthesize 5CoUiO-66, a slightly lower Co content was obtained (3.61% to 2.83%). It could be ascribed to the complexation between metal ions and $–NH_2$ as reported [37]. With no $–NH_2$, it could be harder for UiO-66 to adsorb Co ions before $NaBH_4$ treating than UiO-66-$NH_2$. The UV–vis absorption spectra of the samples were shown in Fig. 2A. After loading of Co, the absorption edge of xCoNU samples were barely changed, which suggest that the reduction process didn't alter the structure of UiO-66-$NH_2$. Due to the deep color of Co species, the absorbance of xCoNU increased with the increasing of Co amount [38]. The $CO_2$ adsorption ability of our catalysts was also investigated. UiO-66-$NH_2$ is reported to have better $CO_2$ adsorption ability than UiO-66 [39, 40], which could be beneficial for $CO_2$ reduction. It was found that after the loading of Co, the $CO_2$ adsorption ability of UiO-66-$NH_2$ was slightly decreased as exhibited in Fig. 2B, which could be ascribed to the partial blocking of micropore during the loading process. Therefore, the enhanced $CO_2$ photoreduction efficiency of 5CoNU could not be attributed to the $CO_2$ adsorption capacity.

The valence states of all elements in NU66 and 5CoNU were verified through X-ray photoelectron spectroscopy (Fig. 3). Compared to NU66, the binding energy of Zr 3d in 5CoNU was slightly decreased, which reflected the increased electron density of Zr by Co loading. The binding energy for O 1s was reduced and the peak width was broadened, which could be ascribed to the formation of Co–O bound. On the contrary, binding energy for N 1s was barely changed, which ruled out the formation of Co–N bound. In Co 2p spectra, the binding energy of Co $2p_{1/2}$ and Co $2p_{3/2}$ were respectively located at 780.5 eV and 796.5 eV, corresponding to $Co^{3+}$ CoOOH species [41, 42], which was reported as a result of insufficient reaction between Co precursor and $NaBH_4$ [43]. According to the TEM and XRD results, there are no Co species particles on xCoNU. Therefore, the Co exists as highly dispersed CoOOH in xCoNU.

$CO_2$ photocatalytic reduction performance of xCoNU was evaluated in a homemade quartz reactor with **Ru** as the absorber. As illustrated in Fig. 4A and Table S1, only CO and $H_2$ were detected to be reductive products. It was found that blank UiO-66-$NH_2$ showed a rather low activity for both CO and $H_2$ generation (Fig. 4A). After loading Co, the CO2PR activity of catalysts was significantly improved compared to the bare UiO-66-$NH_2$, which clearly demonstrated that Co sites could work as the main active centers for $CO_2$ photocatalytic reduction reaction. Notably, the selectivity for CO in all xCoNU samples was not altered and fixed at around 65% (Table S1), which suggest the main active sites in the reaction were the same. The optimistic loading amounts of Co was found to be 3.61 wt% (5CoNU), which exhibited an average CO generation rate of 1.93 mmol $g^{-1}$ $h^{-1}$ (9.67 μmol $h^{-1}$ in 3 h, Fig. 4A) and $H_2$ generation rate of 1.18 mmol $g^{-1}$ $h^{-1}$ in 3 h. The TON for CO was 38.66 with 5CoNU in 3 h, which is 10.2 times higher than that of UiO-66-$NH_2$. It was also observed that catalytic performance of this system was suppressed after 3 h, mainly due to the degradation of **Ru** (Fig. S2). Furthermore, durability test was conducted for 5CoNU in Fig. 4B. It was found that the CO2PR performance of the catalyst can still hold after 5 cycles, suggesting good stability of 5CoNU.

To further explore the charge separation ability of xCoNU series catalysts, room-temperature photoluminescence (PL) and electrochemical impedance spectroscopy (EIS) analysis were performed. After the loading of Co, the impedance of UiO-66-$NH_2$ was decreased, which reflected an improved conductivity (Fig. 5A). Furthermore, as illustrated in Fig. 5B, the main PL emission peak of UiO-66-$NH_2$ at 470 nm was greatly reduced after the loading of Co, demonstrating that the suppressed

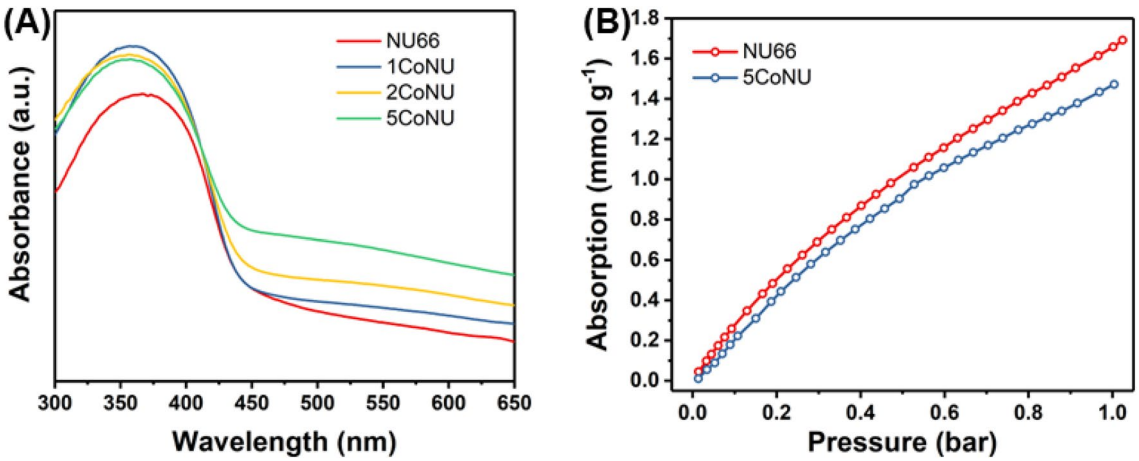


**Fig. 2** **A** UV–Vis DRS spectra of NU66 and xCoNU with different Co content; **B** $CO_2$ adsorption performance of NU66 and 5CoNU at 298 K

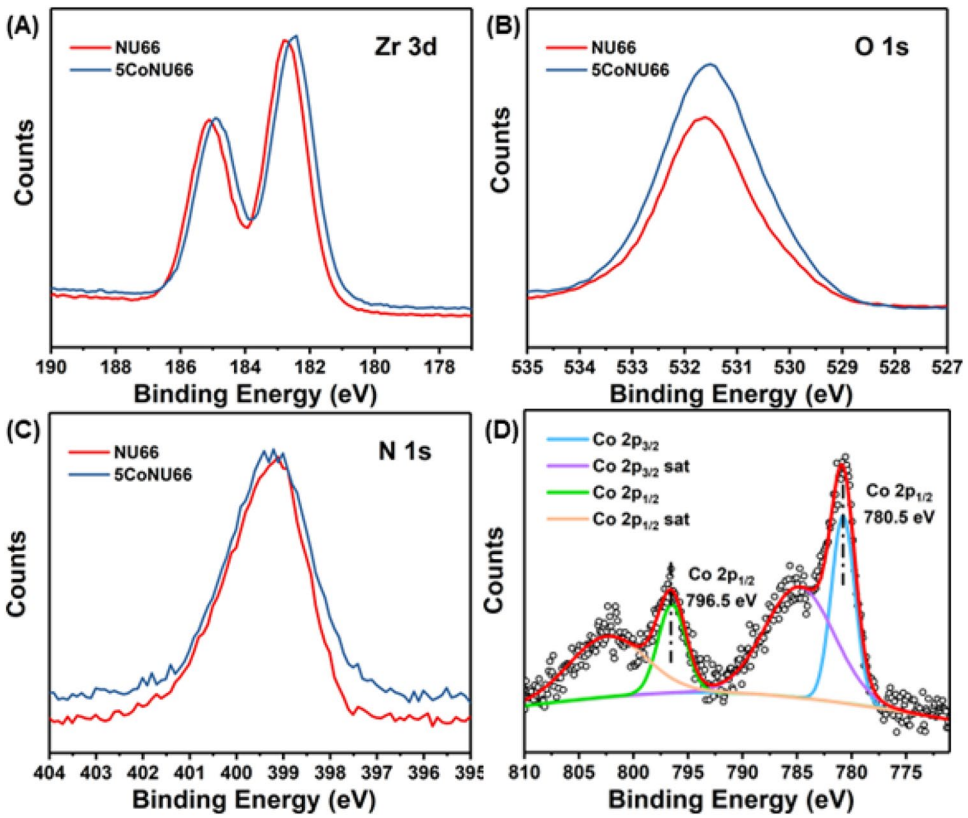


**Fig. 3** XPS **A** Zr 3d spectra, **B** O 1s spectra, **C** N 1s spectra of NU66 and 5CoNU, and **D** Co 2p spectra of 5CoNU

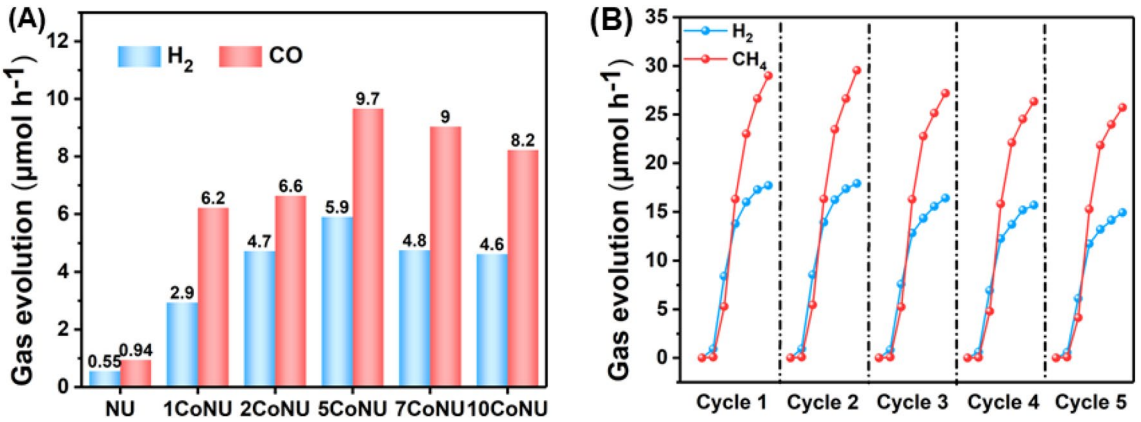


**Fig. 4** **A** $CO_2$ reduction performance of xCoNU samples with different Co content in 3 h; **B** durability experiment of 5CoNU, every cycle lasted for 3 h

recombination of MOF-origined electron–hole pair. Since the absorber **Ru** itself also had strong PL response, we believe it essential to verify if the addition of Co can reduce the total photocarrier recombination within the overall reaction system composed of photocatalyst, **Ru**, and the mixed solution. Figure 5C showed the PL emission of the mix suspension with the same mixture ratio in our CO2PR test. The fluorescence was firstly quenched as the content of Co raised from 0 to 3.61%, which is consisted with the CO2PR result. The lifetime of photoluminescence was also extended (Fig. 5D; Table S3), indicating an enhanced charge separation ability of xCoNU. Additionally, compared with mixed **Ru** and NU66, τ2 of mixed **Ru** and 5CoNU extended better, which reflected a faster electron transition from **Ru** to 5CoNU [44]. Still, the fluorescence intensity increased again after excessive Co loading, suggesting a lower photoinduced carriers separation efficiency. This result demonstrated that overloading of Co may cause the formation of new recombination centers and reduce the reaction efficiency, while proper loading

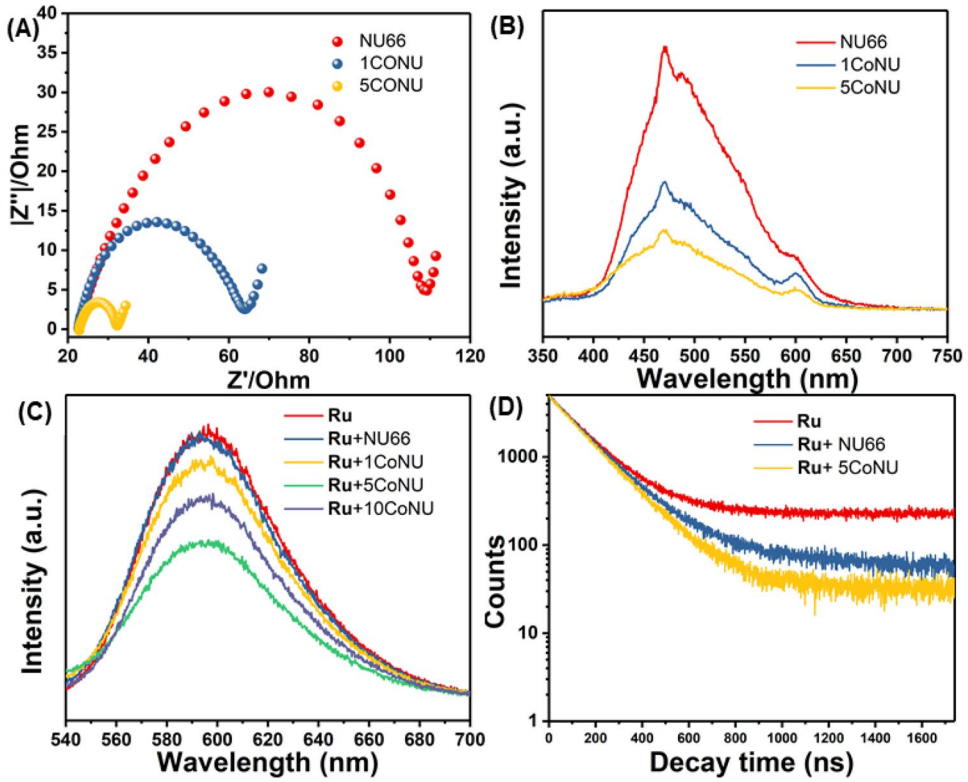


**Fig. 5** **A** EIS spectra of xCoNU; Room-temperature photoluminescence spectra of **B** xCoNU alone and **C** xCoNU with Ru in MeCN solution; **D** TRPL of xCoNU with Ru in MeCN solution

amount of Co could help photoinduced electrons and holes separation within the reaction system.

The influence of dissolvent used for synthesize of 5CoNU was investigated. Results show that there was no difference between samples obtained in nonaqueous solvent, while the sample obtained in aqueous solution showed significant decrease in both $H_2$ and CO generation (Fig. 6A). It could be attributed to the inadequate reaction between Co precursor and $NaBH_4$ due to $NaBH_4$'s self-decomposition in water. As shown in Table 1, 5CoNU obtained from aqueous solution had a lower Co content compared to that from MeCN solution, which confirmed our suspicion.

Series control experiments were employed to explore CO2PR with 5CoNU (obtained in MeCN) under different conditions. As illustrated in Fig. 6B, with no catalyst, only a small amount of gaseous product was detected. In the absence of **Ru** absorber, CO2PR with 5CoNU was also greatly suppressed, and only a small number of products were detected. Only $H_2$ was produced when $CO_2$ was replaced by Ar in the system, which demonstrated that CO came from the reduction of $CO_2$ rather than the

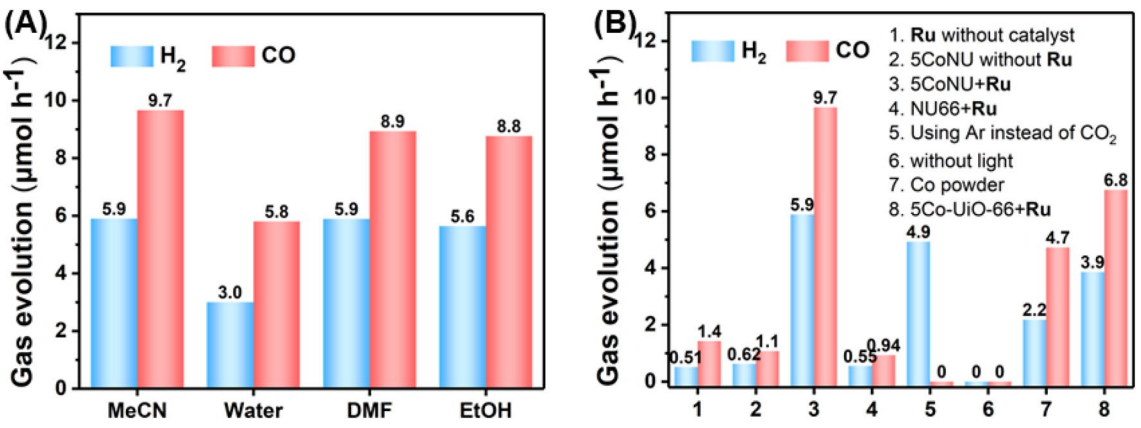


**Fig. 6** **A** Photocatalytic performance of 5CoNUs synthesized in different solutions in 3 h; **B** control experiments, where all samples were synthesized in MeCN

decomposition of other reactants. Also, without light, the reaction was terminated with no product detected, which confirmed the reaction was driven by photoirradiation. These results suggested that photo-electrons from excited **Ru** to active sites on 5CoNU triggered CO2PR in this system. When using Co powder of the same weight as catalyst, only about half the product generation rates were expressed, and the TON for CO was 0.95, which was about fortieth of 5CoNU. As shown in Fig. 1, introduction of UiO-66-$NH_2$ could promote the dispersion of Co sites, which would increase the active Co atoms utilization and promote the CO2PR reaction. A decreased activity was also observed when using UiO-66 as the supporter, which was structurally similar to UiO-66-$NH_2$. Notably, it was confirmed that 5CoUiO-66 had a lower Co loading capacity than 5CoNU, as analyzed by ICP-AES in Table 1. These results suggested that the linker with $–NH_2$ group could help the loading of Co sites, which resulted in a higher photocatalytic reactivity of 5CoNU.

The process for the CO2PR on xCoNU can be illustrated in Fig. 7 based on our experimental results. Upon photoexcitation, the light absorber **Ru** is excited to give electrons and holes. The photoexcited electrons are then transferred to the cobalt sites on xCoNU where $CO_2$ molecule is activated and reduced to CO. The oxidized light absorber is reduced back to **Ru** by the sacrificial reductant TEA to form an entire catalytic cycle. The cobalt sites on xCoNU can work as $CO_2$ active sites and promoted the charge separation within UiO-66-$NH_2$ supporter and between the supporter and absorber, which results in a considerable $CO_2$ conversion efficiency.

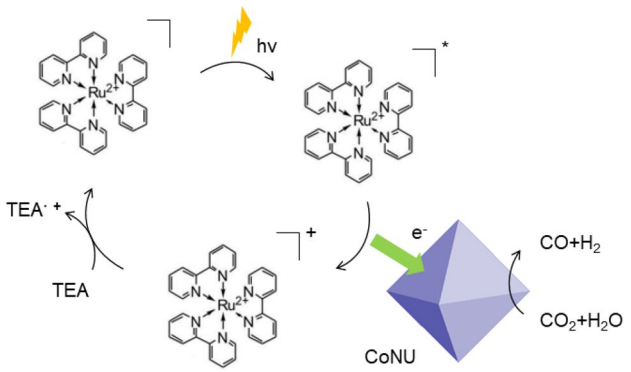


**Fig. 7** Schematic process for the photocatalytic reduction of $CO_2$ to CO using $[Ru(bpy)_3]Cl_2$ as a light absorber and xCoNU as a catalyst

## 4 Conclusions

In summary, UiO-66-$NH_2$ decorated with highly dispersed cobalt has been developed as an efficient catalyst with $NaBH_4$ treating method for $CO_2$ photoreduction. It was proved that the decorated Co atoms could enhance the charge separation and perform as the active centers for $CO_2$ reduction. Our catalyst showed good performance for the photoreduction reaction under simulated solar irradiation. 5CoNU achieved a high CO generation rate of 1.93 mmol $g^{-1}$ $h^{-1}$ and $H_2$ generation rate of 1.18 mmol $g^{-1}$ $h^{-1}$ in 3 h. Compared to Co powder, the TON of 5CoNU was lifted approximately 40 times due to the highly dispersed cobalt. This work provides a simple and convenient method to modify MOFs with metal cocatalyst for photocatalytic application.

**Supplementary Information** The online version contains supplementary material available at https://doi.org/10.1007/s10562-022-04081-5.

**Acknowledgements** This work was supported by National Natural Science Foundation of China (Grant Nos. 21972040, 21773062), Innovation Program of Shanghai Municipal Education Commission (Grant No. 2021-01-07-00-02-E00106), and the Science and Technology Commission of Shanghai Municipality (Grant No. 20DZ2250400).

## Declarations

**Conflict of interest** There are no conflict to declare.

## References

1. Jin J, Yu J, Guo D, Cui C, Ho W (2015) Small 11:5262
2. Kang Q, Wang T, Li P, Liu L, Chang K, Li M, Ye J (2015) Angew Chem Int Ed Engl 54:841
3. Khan IS, Mateo D, Shterk G, Shoinkhorova T, Poloneeva D, Garzon-Tovar L, Gascon J (2021) Angew Chem Int Ed Engl 60:26476
4. Mateo D, Albero J, García H (2019) Joule 3:1949
5. Ran J, Jaroniec M, Qiao S-Z (2018) Adv Mater 30:1704649
6. Li X, Yu J, Jaroniec M, Chen X (2019) Chem Rev 119:3962
7. Dong C, Lian C, Hu S, Deng Z, Gong J, Li M, Liu H, Xing M, Zhang J (2018) Nat Commun 9:1252
8. Dong C, Xing M, Zhang J (2016) J Phys Chem Lett 7:2962
9. Jiang Z, Wan W, Li H, Yuan S, Zhao H, Wong PK (2018) Adv Mater 30:1706108
10. Wang M, Shen M, Jin X, Tian J, Li M, Zhou Y, Zhang L, Li Y, Shi J (2019) ACS Catal 9:4573
11. Van Wyk A, Smith T, Park J, Deria P (2018) J Am Chem Soc 140:2756
12. Chambers MB, Wang X, Ellezam L, Ersen O, Fontecave M, Sanchez C, Rozes L, Mellot-Draznieks C (2017) J Am Chem Soc 139:8222
13. Wang G, He CT, Huang R, Mao J, Wang D, Li Y (2020) J Am Chem Soc 142:19339
14. Liu S, Sun L, Xu F, Zhang J, Jiao C, Li F, Li Z, Wang S, Wang Z, Jiang X, Zhou H, Yang L, Schick C (2013) Energy Environ Sci 6:818

15. Burns TD, Pai KN, Subraveti SG, Collins SP, Krykunov M, Rajendran A, Woo TK (2020) Environ Sci Technol 54:4536
16. Daglar H, Gulbalkan HC, Avci G, Aksu GO, Altundal OF, Altintas C, Erucar I, Keskin S (2021) Angew Chem Int Ed Engl 60:7828
17. Segakweng T, Musyoka NM, Ren J, Crouse P, Langmi HW (2015) Res Chem Intermed 42:4951
18. Zhang FM, Sheng JL, Yang ZD, Sun XJ, Tang HL, Lu M, Dong H, Shen FC, Liu J, Lan YQ (2018) Angew Chem Int Ed Engl 57:12106
19. Guo J, Liang Y, Liu L, Hu J, Wang H, An W, Cui W (2020) Appl Surf Sci 522:146356
20. Crake A, Christoforidis KC, Kafizas A, Zafeiratos S, Petit C (2017) Appl Catal B:Environ 210:131
21. Zheng C, Qiu X, Han J, Wu Y, Liu S, Appl ACS (2019) Mater Inter 11:42243
22. Toyao T, Saito M, Dohshi S, Mochizuki K, Iwata M, Higashimura H, Horiuchi Y, Matsuoka M (2016) Res Chem Intermed 42:7679
23. Feng S, Wang R, Feng S, Zhang Z, Mao L (2018) Res Chem Intermed 45:1263
24. Choi KM, Kim D, Rungtaweevoranit B, Trickett CA, Barmanbek JTD, Alshammari AS, Yang P, Yaghi OM (2017) J Am Chem Soc 139:356
25. Zhong W, Sa R, Li L, He Y, Li L, Bi J, Zhuang Z, Yu Y, Zou Z (2019) J Am Chem Soc 141:7615
26. Hao YC, Chen LW, Li J, Guo Y, Su X, Shu M, Zhang Q, Gao WY, Li S, Yu ZL, Gu L, Feng X, Yin AX, Si R, Zhang YW, Wang B, Yan CH (2021) Nat Commun 12:2682
27. Zhang J-H, Yang W, Zhang M, Wang H-J, Si R, Zhong D-C, Lu T-B (2021) Nano Energy 80:105542
28. Wang X, Chen W, Zhang L, Yao T, Liu W, Lin Y, Ju H, Dong J, Zheng L, Yan W, Zheng X, Li Z, Wang X, Yang J, He D, Wang Y, Deng Z, Wu Y, Li Y (2017) J Am Chem Soc 139:9419
29. Dhakshinamoorthy A, Asiri AM, García H (2016) Angew Chem Int Ed 55:5414
30. Huang H, Shen K, Chen F, Li Y (2020) ACS Catal 10:6579
31. Dong C, Xing M, Zhang J (2016) Mater Horiz 3:608
32. Mu Q, Zhu W, Yan G, Lian Y, Yao Y, Li Q, Tian Y, Zhang P, Deng Z, Peng Y (2018) J Mater Chem A 6:21110
33. Call A, Cibian M, Yamamoto K, Nakazono T, Yamauchi K, Sakai K (2019) ACS Catal 9:4867
34. Zhang H, Wei J, Dong J, Liu G, Shi L, An P, Zhao G, Kong J, Wang X, Meng X, Zhang J, Ye J (2016) Angew Chem Int Ed 55:14310
35. Fu J, Zhu L, Jiang K, Liu K, Wang Z, Qiu X, Li H, Hu J, Pan H, Lu Y-R, Chan T-S, Liu M (2021) Chem Eng J 415:128982
36. Luu CL, Nguyen TTV, Nguyen T, Hoang TC (2015) Adv Nat Sci Nanosci Nanotechnol 6:025004
37. Jamshidifard S, Koushkbaghi S, Hosseini S, Rezaei S, Karamipour A, Jafari rad A, Irani M (2019) J Hazard Mater 368:10
38. Xiao F (2012) Chem Commun 48:6538
39. Cao Y, Zhang H, Song F, Huang T, Ji J, Zhong Q, Chu W, Xu Q (2018) Materials 11:589
40. Strauss I, Chakarova K, Mundstock A, Mihaylov M, Hadjiivanov K, Guschanski N, Caro J (2020) Micropor Mesopor Mat 302:110227
41. Xu Z, Li X, Li J, Wu L, Zeng Q, Zhou Z (2013) Appl Surf Sci 284:285
42. Cao A, Li R, Xu X, Huang W, He Y, Li J, Sun M, Chen X, Kang L (2022) Appl Catal B Environ 309:121293
43. Glavee GN, Klabunde KJ, Sorensen CM, Hadjipanayis GC (1993) Langmuir 9:162
44. Gao C, Chen S, Wang Y, Wang J, Zheng X, Zhu J, Song L, Zhang W, Xiong Y (2018) Adv Mater 30:1704624